AIP | Journal of Applied Physics

A microlens array based on polymer network liquid crystal

Miao Xu, Zuowei Zhou, Hongwen Ren, Seung Hee Lee, and Qionghua Wang

Citation: J. Appl. Phys. **113**, 053105 (2013); doi: 10.1063/1.4790303
View online: http://dx.doi.org/10.1063/1.4790303
View Table of Contents: http://jap.aip.org/resource/1/JAPIAU/v113/i5
Published by the American Institute of Physics.

A microlens array based on polymer network liquid crystal

Miao Xu,[1] Zuowei Zhou,[1] Hongwen Ren,[1,a)] Seung Hee Lee,[1,2] and Qionghua Wang[3]
[1]*Department of Polymer-Nano Science and Technology, Chonbuk National University, Jeonju, Jeonbuk 561-756, South Korea*
[2]*Department of BIN Fusion Technology, Chonbuk National University, Jeonju, Jeonbuk 561-756, South Korea*
[3]*School of Electronics and Information Engineering, Sichuan University, Chengdu 610065, China*

(Received 19 October 2012; accepted 17 January 2013; published online 4 February 2013)

Using UV light to expose a homogeneous cell containing liquid crystal (LC)/monomer mixture through a patterned photomask, we prepared a polymer network liquid crystal (PNLC) microlens array. In each microlens, the formed polymer network presents a central-symmetrical inhomogeneous morphology and LC exhibits a gradient refractive index distribution. By applying an external voltage to the cell, the gradient of the LC refractive index is changed. As a result, the focal length of the microlens can be tuned. Our PNLC microlens array has the advantages of low operating voltage, easy fabrication, and good stability. This kind of microlens array has potential applications in image processing, optical communications, and switchable 2D/3D displays. © *2013 American Institute of Physics*. [http://dx.doi.org/10.1063/1.4790303]

I. INTRODUCTION

Tunable-focus liquid crystal (LC) microlens arrays have been studied intensively in the past years.[1–9] Applications of these microlenses are widely found in image processing, wavefront sensors, optical communications, and switchable 2D/3D displays. Several approaches, such as patterned electrode,[1,6] surface relief profile,[2–5,10–14] polymer network liquid crystal (PNLC),[7,8] polymer dispersed liquid crystal (PDLC),[9,15] and blue phase,[16,17] were demonstrated. Among them, PNLC is much attractive due to the advantages of simple fabrication, low operating voltage, improved phase shift, and reasonable response time. In a PNLC microlens, LC usually presents homogeneous alignment in the formed polymer network. With an externally applied voltage, a gradient refractive index distribution is induced. As a result, the focal length of the PNLC microlens can be tuned.

To obtain a PNLC microlens, a convenient way is to use a UV light to expose a homogeneous cell containing LC/monomer mixture. The UV light intensity distribution, which plays an important role for forming the PNLC, is nonuniform. Two types of UV light have been employed: a laser beam with Gaussian-shaped intensity profile[7] and a uniform UV light passing through a hole-array patterned photomask.[8] The latter method is much simple and suitable to obtain a microlens array. When a UV light passes through a tiny hole, the diffracted light intensity presents a Gaussian-shaped profile. When such a light is used to expose the mixture of LC/monomer, the photo-polymerization only occurs in the UV exposed region. Monomers in the cell will shift to the UV exposed region. As a result, the monomer concentration in the UV exposed area is enhanced and the formed polymer network becomes dense. Due to this reason, the external voltage for driving the PNLC microlens is increased and it is rather limited to increase the gradient of the PNLC microlens.

In this paper, we report a tunable-focus PNLC microlens array which was prepared using UV light to expose a homogeneous LC/monomer mixture through a photomask. The photomask was made by patterning a chromium layer with a circular spot array on a glass plate surface. When a uniform UV light passes through the photomask, the diffracted light intensity by each circular spot is inhomogeneous. Such a UV light can polymerize the monomers with gradient polymer network and the formed PNLC exhibits a lens-like character. When a voltage is applied to the PNLC, the focal length of the lens is changed. In comparison with previous results, our PNLC microlens has the advantages of wide focal-length tunability, low operating voltage, and good stability.

II. MECHANISM OF FORMING GRADIENT PNLC

A. Basic diffraction theory

When a laser beam meets a circular obstruction, diffraction takes place. In the center of the shadow cast by the obstruction, a Poisson spot as well as surrounding annuli are generated. According to Fresnel's diffraction, the intensity profile of this spot can be expressed by[18,19]

$$I \propto J_o^2\left(\frac{\pi Dr}{\lambda b}\right), \tag{1}$$

where J_0 is the Bessel function of the zeroth order, D is the diameter of the circular disk, r is the radial position on the viewing screen from the optical axis, λ is the wavelength, and b is the distance between black disk and screen. Such a diffraction pattern has been proved by numerous simulations and experimental results.[19–21] In comparison to the formed bright rings, most of light energy concentrates on the Poisson spot (also called 0th order ring). The intensity distribution of the Poisson spot presents a parabolic-like profile. Similarly, when an incoherent UV light is used to illuminate the black disk, it is diffracted too. Close to the optical axis position of the received screen, the UV light intensity is the highest. Away from the optical axis, the light intensity has a tendency

a)Email: hongwen@jbnu.ac.kr.

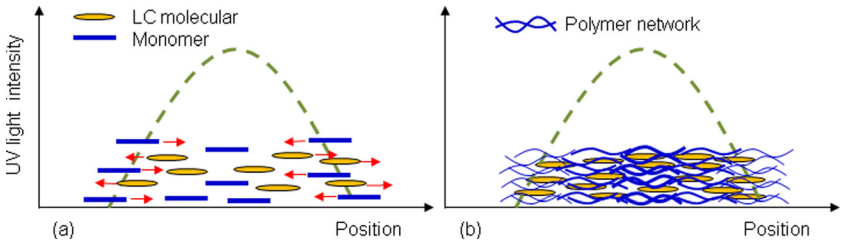

FIG. 1. Mechanism of forming a gradient PNLC: (a) diffusion of LC and monomers during UV exposure and (b) the formed polymer network after UV exposure.

to decrease. Due to incoherence and broadband spectrum, the diffracted UV light intensity behind each circular disk will change smoothly with a gradient.

B. Phase separation mechanism

When an inhomogeneous UV light is used to expose a homogeneous cell containing LC and monomer mixture, phase separation and kinetic diffusion take place in the mixture. The phase separation mechanism is depicted in Fig. 1. Before UV exposure, the monomer concentration in the LC bulk is uniform and LC presents homogeneous alignment. When an inhomogeneous UV light is used to expose the mixture (Fig. 1(a)), the polymerization preferentially starts in the stronger UV region. The consumption of monomers in this region lowers their chemical potential. To balance the decreased potential, the uncured monomers in the weaker UV region have to diffuse towards the stronger UV region. On the other hand, LC molecules are UV stable and not consumed. They shift to the weaker UV region because of higher chemical potential.[22] Due to this kinetic diffusion, the density of monomer is richer in higher UV intensity region and LC is richer in weaker UV region. After polymerization, a denser (looser) polymer network is formed in the stronger (weaker) UV intensity region. Since the intensity of UV light changes continuously, the formed PNLC presents a gradient density distribution (Fig. 1(b)). If the morphology of the PNLC is central symmetrical, then the PNLC behaves a lens character. Based on this mechanism, various photonic devices, such as composite LC film,[23] surface profile LC lens,[24] and holographic LC grating have been developed.[22,25]

III. DEVICE FABRICATION

To fabricate a gradient PNLC as depicted in Fig. 1(b), the material system consisting of 97 wt. % of nematic LC MLC-2140 ($\Delta n = 0.253$, $n_o = 1.516$, $\Delta\varepsilon = 47.6$, Merck) and 3 wt. % of monomer RM-257 (diacrylate monomer mixed with ~1 wt. % photoinitiator) was prepared. The monomer RM-257 is a rod-like structure with reactive double bonds at both sides, as shown below.

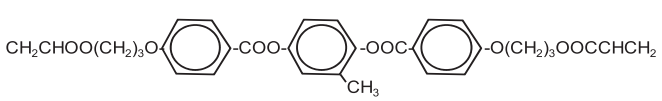

Similar to a nematic LC, RM-257 is a LC monomer and it exhibits high reorientation order in the LC host.

The mixture was injected into a homogeneous empty cell in the isotropic state. The inner glass substrate surfaces of the cell are overcoated with indium-tin-oxide (ITO) electrode, followed by polyimide (PI) alignment layers. The PI layers were buffed in antiparallel directions. The cell gap and the thickness of the glass substrate are ~15 μm and 1.1 mm, respectively. After the cell was cooled slowly to room temperature, LC and the monomer present a homogeneous alignment due to PI surface anchoring.

To obtain a UV light with inhomogeneous intensity distribution, a photomask with a chromium-spot array pattern on a glass plate surface was chosen as the obstruction. Figure 2(a) shows the arrangement of the patterned photomask taken using an optical microscope. The diameter of each circular-spot is 150 μm. The LC cell was attached to the photomask and a uniform UV light (~12.5 mw/cm^2 Model SP-9, Korea) is used to expose the cell from the left side, as shown in Fig. 2(b). Because the thickness of the glass substrate is much larger than the diameter of the black disk (over ~7.3×), the shadow area of the disk can be occupied by the left glass substrate of the cell and the UV Poisson spot can reach the LC/monomer layer. As we described above, the UV light can cause the LC/monomer to form an inhomogeneous PNLC. In this experiment, the cell was cured for ~20 min.

IV. RESULTS AND DISCUSSION

To evaluate the cured cell, a convenient way is to inspect the cell using the optical microscope. First, we observed the color change of the cell with different voltages. The cell was placed between crossed polarizers. The rubbing direction of the cell was oriented at 45° with respect to the axis of the linear polarizer and the analyzer. Five photographs at different voltages were taken, as shown in Fig. 3.

At $V = 0$, a circle array can be observed clearly (Fig. 3(a)). These circles are the regions formed behind the black spots of the photomask after UV exposure. The area of each circle presents almost a uniform (greenish) color. This implies that LC exhibits homogeneous alignment. The diameter of each circle is ~200 μm. The distance of the adjacent circles is 60 μm. When an external voltage is applied to the cell and increased slowly, the cured spots become noticeable. Meanwhile the color change starts from the borders and gradually moves to the center. This indicates that the threshold voltage in the spot center is higher than that at the borders. The threshold is mainly dependent on the formed polymer network. In the central region of each spot, the formed polymer network is denser. At the borders, the formed polymer network is looser. At $V = 1.5\ V_{rms}$, the color change is obvious (Fig. 3(b)). Such a result confirms the expected gradient of the PNLC shown in Fig. 1(b). At $V = 3\ V_{rms}$, the color change of each spot is much noticeable (Fig. 3(c)). As the voltage is increased continuously, the color change becomes dull. This is because most LC

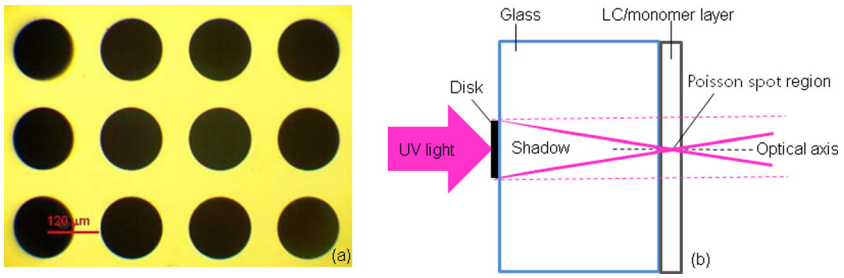

FIG. 2. (a) The photomask taken using an optical microscope. The black circular spot (diameter-$= 150\,\mu$m) is the chromium layer patterned on a glass plate surface. (b) Experimental setup for preparing a PNLC microlens array. The thickness of the glass substrate and the diameter of the disk are not drawn in scale.

directors in the polymer network are reoriented perpendicular to the substrates. Under such a circumstance, the refractive index profile is much flattened. The color changes at $V = 5\,V_{rms}$ (Fig. 3(d)) and $V = 6\,V_{rms}$ (Fig. 3(e)) confirm such a result. To visually observe the dynamic color change, a video showing the color change with different voltages is given in Fig. 3(e) as well. The voltage applied to the cell is gradually increased (decreased) from 0 (10) to 10 (0) V_{rms}. Two cycles are given. The response time impacted by 10-V squared voltage pulse was estimated to be $\sim$30 ms. Our cell has been cyclically driven for hundred times, it could recover to its original alignment state well after removing the voltage. Such a result implies that the formed PNLC is stable at low driving voltage.

To clearly observe the phase separation morphology of the LC cell, we magnified one of the circular spot in the $V = 10\,V_{rms}$ state and focused on the surface of LC layer. Owing to the external voltage, most LC molecules are reoriented along the electric field direction. The LC molecules only strongly anchored by the polymer network surface will not be affected. The surface-anchored LC molecules still generate some phase retardation. Due to this reason, the residual color can easily help us to inspect the formed polymer network. Fig. 3(f) shows the observed morphology. Polymer is rich in the center and LC is rich at the border. Compared to the expected morphology shown in Fig. 1(b), indeed, a gradient polymer network (or LC) has been obtained.

Since the formed polymer network is fixed, only LC can be reoriented by the applied voltage. Theoretically, the phase shift and the refractive index change are expressed by[26]

$$\Delta\varphi = \frac{2\pi\, d\, \delta n}{\lambda}, \tag{2}$$

where d is the LC layer thickness, δn is the refractive index difference between the lens center and the border, and λ is the light wavelength. Figure 4 shows the phase profiles of the homogeneous PNLC operated at $V = 0$, 2, and 6 V_{rms}, respectively. The phase profile is due to the refractive index change of the LC. At $V = 0$, the phase profile is almost flat because LC in the polymer network presents quasi-homogeneous alignment. The effect of LC concentration fluctuation on the phase shift is negligible. At $V = 2\,V_{rms}$, the phase profile presents a bell shape. At $V = 6\,V_{rms}$, the phase loss is severe and the phase profile becomes much flat.

From the changed phase profile, each circular spot behaves as an adaptive microlens. To evaluate the lens performance and measure the focal length, we use a laser beam profiler (BGS-USB-SP503, Newport) to analyze the beam focusing of the PNLC cell. The experimental setup is sketched in Fig. 5. The sample was mounted on a linear metric stage. A collimated linearly-polarized He–Ne laser beam ($\lambda = 633$ nm) was used to illuminate the sample. The beam intensity was controlled by a neutral density filter (DF) and the transmitted light was collected by an imaging lens (L_2)

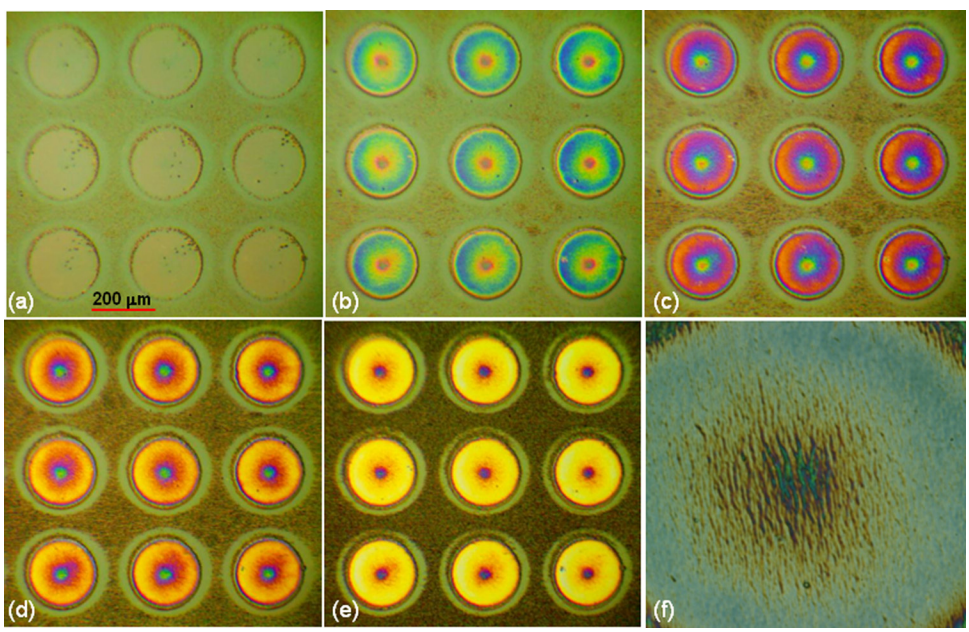

FIG. 3. Photographs of the PNLC cell at different voltages (a) $V = 0$, (b) $V = 1.5\,V_{rms}$, (c) $V = 3\,V_{rms}$, (d) $V = 4\,V_{rms}$, (e) $V = 6\,V_{rms}$, and (f) the magnified morphology at $V = 10\,V_{rms}$. A video (media-1) showing the color change with voltage is given in Fig. 3(e) (enhanced online) [URL: http://dx.doi.org/10.1063/1.4790303.1].

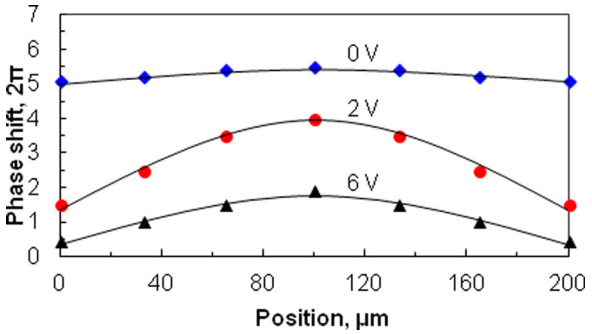

FIG. 4. Phase profiles of one pixel at $V = 0$, 2, and 6 V_{rms}, respectively.

and detected by the beam profiler. The cell was driven by a computer controlled LABVIEW data acquisition system.

To characterize the light focusing properties of the PNLC microlens array, we measured the 3D profiles of the outgoing beams. The intensity profiles were measured at $V = 0$, 1.5, 2.2, and 10 V_{rms}, and results are shown in Fig. 6. At $V = 0$, there is no light focusing effect for each microlens except a little noisy background (Fig. 6(a)). At null voltage state, LC in the polymer network exhibits a quasi-homogeneous alignment and the gradient of refractive index distribution in each microlens is very small. In comparison to the microlens size, the focal length of each microlens is at infinity. As the voltage is increased to $V = 1.5$ V_{rms} (Fig. 6(b)), an array of intensity profile is clearly observed. Because the incident laser beam presents the Gaussian-shaped intensity distribution, the peak intensities are not uniform. Here, we choose one microlens (indicated by letter p) for measurement. For light passing through this microlens, the measured intensity of the peak reaches ~2300 cnts. The increased intensity implies that the focal length of the microlens is decreased due to the increased gradient refractive index of LC in the polymer network. At $V = 2.2$ V_{rms}, the focusing effect of this microlens manifests (Fig. 6(c)). The measured intensity of the peak exceeds ~4100 cnts. As the voltage is further increased, the peak intensity of the outgoing beam tends to decrease. At $V = 10$ V_{rms}, the peak intensity (~2370 cnts) drops largely (Fig. 6(d)). This is because the LC directors in the polymer-rich are highly reoriented along the electric field direction. The gradient of the refractive index distribution is much flattened. As a result, the focal length of the microlens increases and the measured light intensity at the beam profiler focal plane decreases.

The voltage-dependent focal length of the microlens is plotted in Fig. 7. At a given voltage, each microlens in the array gives the same focal length due to the same PNLC morphology. Here, we still choose the microlens (indicated

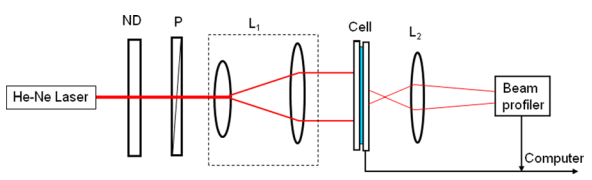

FIG. 5. Experimental setup for characterizing the PNLC microlens array. ND = neutral density filter, L_1 = the lens system for beam expending, and L_2 = imaging lens.

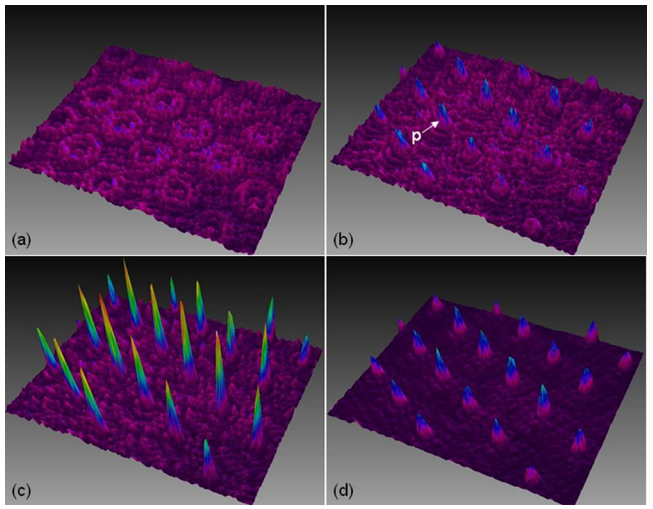

FIG. 6. Images of the laser beam intensity profile passing through the PNLC microlens array at (a) $V = 0$, (b) $V = 1.5$ V_{rms}, (c) $V = 2.2$ V_{rms}, and (d) $V = 10$ V_{rms}, respectively.

by p) for measurement. At $V = 0$, the focal length is very long ($f \sim \infty$ in comparison to its size) due to the very small gradient of refractive index profile. When the applied voltage increases to $V = 1$ V_{rms}, the focal length decreases largely. At $V = 2$ V_{rms}, the focal length becomes the shortest ($f \sim 3.55$ mm). Such result implies that the gradient of the PNLC microlens is the largest. When the applied voltage is increased continuously, the focal length of the microlens has a tendency to increase. This is due to the LC directors inside the polymer network are reoriented by the electric field so that the gradient of the PNLC decreases. The error bars shown in Fig. 7 result from the uncertainty in determining the beam waist. From Fig. 7, the focal length can be widely tuned by a low voltage.

Theoretically, the focal length of the LC microlens can be calculated using the below expressed by[27]

$$f = \frac{r^2}{2d\delta n}, \tag{3}$$

where r is the radius of lens aperture. From Eq. (3), δn can be changed by the external voltage, so that the focal length f is tuned. According to the phase profile given in Fig. 4, the focal length of the microlens could be calculated using Eq. (3) as well. The calculated focal length should match the focal length measured in Fig. 7. According to Eq. (3), the shortest focal length of the microlens is dependent on the

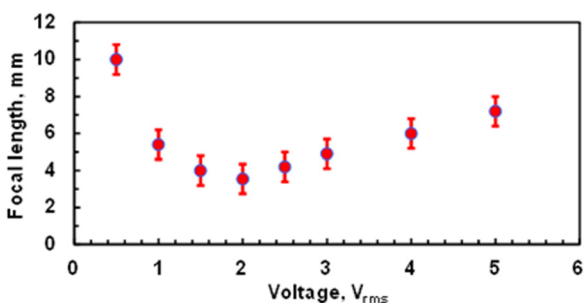

FIG. 7. Voltage-dependent focal length of a PNLC microlens.

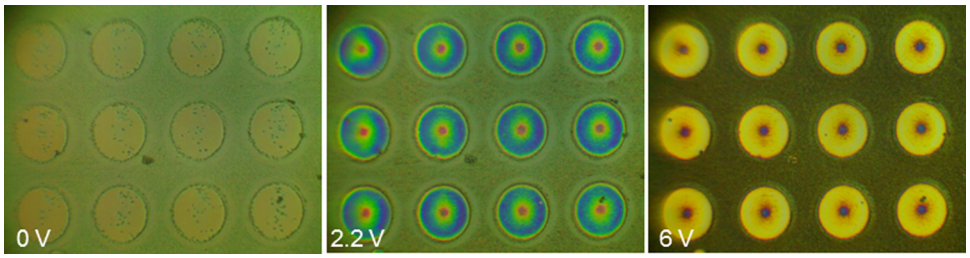

FIG. 8. The photographs of the PNLC microlens at different voltages after impacting at 80 °C for 3 h.

cell gap, the birefringence of LC, and the radius of the lens aperture. For the microlens with a fixed aperture, several ways can be used to enhance the focal power of the microlens ($P = 1/f$), for example, increase the cell gap, use a high birefringence LC material, and optimize the UV intensity profile for curing the cell.

From Fig. 7, the focal length of the microlens was measured at room temperature. According to Haller's approximation, as the temperature increases, the birefringence of LC decreases gradually.[28] There is no doubt that the effective birefringence (δn) of our LC microlens obeys such an approximation. From Eq. (3), the focal length of the microlens will have a tendency to increase as δn decreases. As the temperature is increased to the LC clear point, $\delta n = 0$. As a result, the focal length is calculated to be $f \sim \infty$. For practical applications, the temperature effect on the stability of the PNLC should be evaluated. To study the stability of the PNLC over temperature, the cell was heated at 80 °C in an oven for 3 h. Such a high temperature is close to the LC clearing point. After heating, the PNLC microlens array was analyzed using the optical microscope. Figure 8 shows the color change of the microlenses at three different driving voltages. In comparison with the results shown in Fig. 3, the performance of the PNLC microlens array does not become worse. After removing the voltage, the PNLC could fully return to its original state. Our results show that the formed PNLC is still stable even after impacting at 80 °C for 3 h.

From Eqs. (2) and (3), the phase retardation or the birefringence of LC is dependent on the wavelength of the incident light. For different wavelengths, the focal length will be different. Therefore, chromatic (or spherical chromatic) aberration should be the main shortcoming of a LC lens. Due to this reason, a LC lens or microlens array is suitable for focusing monochromatic light or laser light. Especially, a LC microlens array is suitable for switchable 2D/3D displays without the concern of chromatic aberration. This is because color filters imbedded in the display device provide monochromatic light to these lenses.

From Figs. 2 and 3, the distance of the neighboring microlenses can be affected by two factors: the pattern of the photomask and the distance from the photomask to the LC layer. According to optical diffraction theory, the size of each black disk should be controlled in micro scale, so that light diffraction can occur behind each disk. A circular disk with macro-sized aperture could not effectively diffract light. Although the Poisson spot (like a beam waist) exhibits a parabolic-like intensity profile with the highest gradient, its size is too small. To increase the aperture size of each microlens during UV exposure, the distance from the disk to the LC layer should be fairly optimized. Normally the aperture of the formed PNLC microlens is smaller than that of its circular disk (depicted in Fig. 2(b)), the distance of the neighboring microlens is smaller than the gap of the adjacent disks.

Depending on the patterns of the photomask, other adaptive photonic devices, such as Fresnel-zone lens or lenticular microlenses, can be prepared as well. The latter is suitable for switchable 2D/3D displays.[29,30] Comparing with conventional PNLC microlens, the focal length of our PNLC microlens can be widely tuned with low driving voltage. Although only ~3 wt. % diacrylate monomer is used in the LC mixture, the formed PNLC microlens array presents good stability, reasonably response time, and negligible light scattering.

V. CONCLUSION

We demonstrated a PNLC microlens array. The microlens array was prepared using UV light to expose a homogeneous cell containing the mixture of LC/diacrylate monomer through a patterned photomask. The fabrication process is simple and the microlens array can be easily prepared. Due to the non-uniform polymer network distribution, each PNLC microlens has a gradient refractive index distribution called gradient PNLC. When an external voltage is applied to the cell, the gradient of the PNLC microlens is changed. As a result, the focal length of the microlens is tuned. Low operating voltage, reasonable dynamic response, and good stability are the advantages of our PNLC microlenses. To enhance the gradient of PNLC microlenses, two simple methods can be considered: increase the cell gap and choose a LC with larger birefringence. This PNLC microlens array has attractive applications in image processing, optical communications, and switchable 2D/3D displays.

ACKNOWLEDGMENTS

This work was supported by the National Research Foundation (NRF) of Korea, the Korea-China Joint Research Program (2012-0004814), and partially supported by National Research Foundation of Korea under Contract No. 2010-0021680

[1]T. Nose and S. Sato, Liq. Cryst. **5**, 1425 (1989).
[2]L. G. Commander, S. E. Day, and D. R. Selviah, Opt. Commun. **177**, 157 (2000).
[3]H. S. Ji, J. H. Kim, and S. Kumar, Opt. Lett. **28**, 1147 (2003).
[4]Y. Choi, J.-H. Park, J.-H. Kim, and S.-D. Lee, Opt. Mater. **21**, 643 (2003).
[5]H. R. Stapert, S. del Valle, E. J. K. Verstegen, B. M. I. van der Zande, J. Lub, and S. Stallinga, Adv. Funct. Mater. **13**, 732 (2003).
[6]T. Nose, S. Masuda, S. Sato, J. Li, L.-C. Chien, and P. J. Bos, Opt. Lett. **22**, 351 (1997).

[7]V. V. Presnyako, K. E. Asatryan, and T. V. Galstian, Opt. Express **10**, 865 (2002).
[8]H. Ren, Y.-H. Fan, Y.-H. Lin, and S.-T. Wu, Opt. Commun. **230**, 267 (2004).
[9]H. Ren, Y. H. Fan, Y. H. Lin, and S. T. Wu, Opt. Commun. **247**, 101 (2005).
[10]Y.-H. Fan, H. Ren, X. Liang, H. Wang, and S.-T. Wu, J. Disp. Technol. **1**, 151 (2005).
[11]Y. Choi, H.-R. Kim, K.-H. Lee, Y.-M. Lee, and J.-H. Kim, Appl. Phys. Lett. **91**, 221113 (2007).
[12]H. T. Dai, Y. J. Liu, X. W. Sun, and D. Luo, Opt. Express **17**, 4317 (2009).
[13]M. Reznikov, Yu. Reznikov, K. Slyusarenko, J. Varshal, and M. Manevich, J. Appl. Phys. **111**, 103118 (2012).
[14]G. Xiong, G. Han, C. Sun, H. Xu, H. Wei, and Z.-Z. Gu, Adv. Funct. Mater. **19**, 1082 (2009).
[15]J.-H. Na, S. C. Park, S.-U. Kim, Y. Choi, and S.-D. Lee, Opt. Express **20**, 864 (2012).
[16]Y.-H. Lin, H.-S. Chen, H.-C. Lin, Y.-S. Tsou, H.-K. Hsu, and W.-Y. Li, Appl. Phys. Lett. **96**, 113505 (2010).
[17]Y. Li and S.-T. Wu, Opt. Express **19**, 8045 (2011).
[18]E. Hecht, *Optics*, 4th ed. (Addison-Wesley, San Francisco, 2001).
[19]J. E. Harvey and J. L. Forgham, Am. J. Phys. **52**, 243 (1984).
[20]W. R. Kelly, E. L. Shirley, A. L. Migdall, S. V. Polyakov, and K. Hendrix, Am. J. Phys. **77**, 713 (2009).
[21]M. Brunel, D. Mgharaz, and S. Coetmellec, Opt. Express **16**, 10390 (2008).
[22]A. Y.-G. Fuh, T.-C. Ko, M.-S. Tsai, C.-Y. Huang, and L.-C. Chien, J. Appl. Phys. **83**, 679 (1998).
[23]V. Vorflusev and S. Kumar, Science **283**, 1903 (1999).
[24]I. Kim, J. H. Kim, D. Kang, D. M. A. Kooijman, and S. Kumar, J. Appl. Phys. **92**, 7699 (2002).
[25]R. L. Sutherland, L. V. Natarajan, V. P. Tondiglia, and T. J. Bunning, Chem. Mater. **5**, 1533 (1993).
[26]S. T. Wu and D. K. Yang, *Reflective Liquid Crystal Displays* (Wiley, New York, 2001).
[27]S. T. Kowel, D. S. Cleverly, and P. G. Korneich, Appl. Opt. **23**, 278 (1984).
[28]I. Haller, Prog. Solid State Chem. **10**, 103 (1975).
[29]Y.-P. Huang, C.-W. Chen, and Y.-C. Huang, J. Disp. Technol. **8**, 650 (2012).
[30]M. Krijin, S. T. de Zwart, D. de Boer, O. H. Willemsen, and M. Sluijter, J. Soc. Inform. Disp. **16**, 847 (2008).